Role of Molecular Orientation and Surface Relaxation on Vapor Growth Shape of Molecular Crystals

ARTICLE *in* CRYSTAL GROWTH & DESIGN · FEBRUARY 2012

Impact Factor: 4.89 · DOI: 10.1021/cg201047k

3 AUTHORS, INCLUDING:

Manoj Kumar Singh
Raja Ramanna Centre for Advanced Technology
18 PUBLICATIONS **96** CITATIONS
SEE PROFILE

Arup Banerjee
Raja Ramanna Centre for Advanced Technology
79 PUBLICATIONS **693** CITATIONS
SEE PROFILE

CRYSTAL GROWTH & DESIGN

Article

pubs.acs.org/crystal

Role of Molecular Orientation and Surface Relaxation on Vapor Growth Shape of Molecular Crystals

M. K. Singh,*[,†] Arup Banerjee,[‡] and P. K. Gupta[†]

[†]Laser Materials Development and Devices Division, [‡]BARC Training School at RRCAT, Raja Ramanna Centre for Advanced Technology, Indore, India 452013

ABSTRACT: We report periodic ab initio total energy calculations to predict equilibrium morphology of molecular crystals. The approach is based on the adsorption of molecules upon the underlying crystal surfaces rather than the attachment of two-dimensional slices of thickness of interplanar distance. It takes into account the effect of molecular orientation and surface relaxation of the habit faces on the molecular attachment energy. The approach has been successfully applied to the case of urea and β-succinic acid crystals to calculate equilibrium shapes from the vapor phase. Hartree−Fock and density functional theory have been employed to obtain the atomic structure of different slices and molecular attachment energies. The relaxed morphologies obtained using the Hartree−Fock method yield good agreement with the experimental observations. Observed polar growth morphology of urea crystal has been discussed particularly in the context of different atomic environments of (111) and $(\overline{1}\overline{1}\overline{1})$ faces.

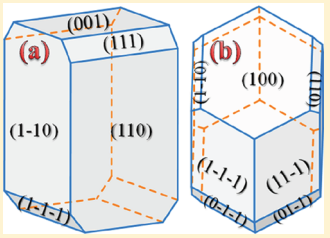

1. INTRODUCTION

The study and manipulation of the forms of crystals have attracted immense attention of artists and academicians equally since the Bronze Age.[1] Though human fascination with crystals is timeless, the mechanism of crystal growth at the atomic scale is still not entirely clear. The relationships between the crystallization forms and its internal structure have captured the interest of scientists long before the crystal structure could be determined from diffraction data. Scientists are eager to understand the physical mechanism by which crystals grow into different shapes. This will enable the crystal grower to manipulate the crystallization processes to obtain a desired shape of crystals. The prediction of growth morphology is of great relevance in many industrial processes and has a direct impact on the separation efficiency and the stability of crystalline chemicals, the bioavailability and the effective delivery of drugs, etc.

A relationship exists between equilibrium morphology and crystal structure. Initial attempts along this direction were made by Bravais (1866), Friedel (1907), and Donnay and Harker (1937) collectively known as BFDH model.[2] The model states that the larger the interplanar spacing, d_{hkl}, the more prominent the face. It takes into account the crystal lattice and its symmetry by reducing the growth slices at faces containing a screw axis or a glide plane. In 1955, a significant contribution was made by Hartman and Perdok (HP)[3] and later modified by Hartman and Bennema,[4] who developed the idea of strong bonds in their periodic bond chain (PBC) theory, connected nets, and roughening to predict external shape of a crystal. A series of contributions by Hartman and Bennema[4] provided the attachment energy (AE) model, which was designed to realize the significance of nonbonded energies in morphology prediction. The development of the AE model was an important milestone in the prediction of crystal morphology. The AE models often make good predictions for crystals that are grown from the vapor.[4−6]

However, these models do not take into account the molecular orientation, surface scaling factor,[7] and relaxation of the habit faces.[8] The relaxation of the crystal faces plays an important role in calculating the growth rates and morphology as the atomic structure at the outermost boundary is believed to control the growth mechanism of the crystal. The molecular attachment energy (MAE) depends on their arrangement in the slices, and thus the influence of molecular orientation on the attachment energy should also be taken into consideration. The predictive power of HP model is limited primarily because the AE of slice is considered as a habit controlling factor without considering the details of molecular anisotropy in the crystal faces. It is thus logical to develop a growth model based on the modified attachment energies. The modified attachment energies should take into account the effect of molecular orientations and surface relaxation on habit controlling energetics, and that is precisely what we have attempted in this paper. We note here that in a series of papers by Strom et al.[9] a graph theoretic approach has been utilized to develop the modern version of the HP model which indirectly takes into account the effect of the surface relaxation on growth morphology.

In this article, we present the results for equilibrium morphologies of urea and β-succinic acid crystals by calculating MAE, which takes into account the effect of molecular orientations and surface relaxation of the crystal faces. We have employed periodic ab initio total energy calculations to obtain atomic structure of various faces and habit controlling energetics of the above crystals. The calculations of unrelaxed

Received: August 12, 2011
Revised: November 15, 2011
Published: December 1, 2011

and relaxed MAE have been carried out in order to investigate the role of surface relaxation. The unrelaxed (relaxed) MAE is the energy released when an unrelaxed (relaxed) molecule is adsorbed on the crystal surface. The vapor grown shapes of urea[7,10−15] and β-succinic acid[16−19] crystals have been extensively studied by using the HP model based on semi-empirical potential due to their simple molecular structures. Docherty et al.[11] and Boek et al.[12] have considered only experimentally observed faces and did not consider surface relaxation for calculating the shape of the urea crystal. On the other hand, George et al.[10] have considered the other than experimentally observed faces to calculate relaxed and unrelaxed equilibrium shapes, but they predicted that the appearance of the (101) and (200) faces and the morphological importance of the (111) face was severely underestimated.

The concept of MAE used in the present paper to predict equilibrium morphology of urea crystal was also used by Bisker-Leib et al.[13] They had calculated modified attachment energies of a reference urea molecule of M1 orientation by summing all the interactions outside a stoichiometric slice up to a limiting radius and then repeated the calculation for the second urea molecule of M2 orientation. The morphology obtained from their modified attachment energies of the molecules showed an improvement over earlier calculations. The methodology of their calculation thus takes into account the molecular anisotropy in the faces of urea crystal. Borc et al.[20] have calculated energies of building units of different orientations to obtain the surface morphology of ionic crystals. Liu and Bennema[7] have utilized the concept of effective growth unit which in turn depends on molecular orientation to calculate the growth shape of molecular crystal. They were the first to model in a systematic way the shape of crystals grown from solution by performing complex molecular dynamic and/or Monte Carlo simulations. They have carried out molecular dynamic simulations to produce the genuine interfacial structure in different crystallographic orientations. However, they have considered only experimentally observed faces to calculate growth morphology of the urea crystal. Morphological prediction of succinic acid crystal has also been widely studied, but none of them has considered (101) and other higher index faces for calculating growth morphology. Our vapor growth shape calculation is based on the simple assumption that the growth units directly adsorb on the crystal surfaces for their growth. On the basis of our calculations, we show that the results obtained by us yield a detailed picture of energetics of solid−solid interactions at the crystal surface, which we find to be useful in elucidating the mechanism of crystal growth at the molecular scale.

2. METHODOLOGY

Recently, it has been shown that monomers or dimers of the molecule are adsorbed during the growth of $ZnCd(SCN)_4$ crystal.[21] Motivated by this study, we present a molecular scale crystal growth model to determine growth morphology. Accordingly, the crystal growth occurs due to the adsorption of building units (BUs) from the vapor phase rather than the attachment of a slice of one d_{hkl} thickness upon the crystal surfaces. The BUs can be described as the smallest cluster (a molecule, complexes, or ions) occurring in the vapor phase and adsorbing upon the crystal surfaces during crystallization. In the case of molecular crystals, the BU can be a monomer or a dimer, but in the present paper we have considered that BUs are monomers. The concept of BU should not be confused with the concept of an asymmetric unit, which is the smallest structural unit that upon translation in space according to the symmetry operations will reproduce the periodic structure of the crystal. The BU reorients itself according to the atomic structure of the face before getting incorporated into a crystal face.

According to HP model, the attachment energy, E_{AE}^{hkl}, of a slice is mathematically expressed as[3,4]

$$E_{AE}^{hkl} = \frac{1}{2}(E_{latt} - E_{slice}^{hkl}) \tag{1}$$

where E_{latt} and E_{slice}^{hkl} are lattice and slice energies, respectively. The factor $^1/_2$ is placed in eq 1 because a slice has two surfaces.[16] The energy released per mole on the formation of a new elementary growth layer, called a slice, with a thickness of d_{hkl}, is the slice energy, E_{slice}^{hkl}, while the energy released per mole on the attachment of a slice on an existing crystal face is the attachment energy, E_{AE}^{hkl}. The lattice energy, E_{latt}, is the energy calculated by summing all nonbonded interactions for the entire, perfect crystal. The lattice energy of organic crystal depends on the molecular conformers.[22] To formulate the crystal growth process at the molecular scale from the vapor phase, we can decompose lattice energy into two terms:[23]

$$E_{latt} = E_{condensation} + E_{conformation} \tag{2}$$

with the $E_{condensation}$ term referring to the condensation of molecules from the vapor phase, but with the same conformation as in the bulk crystal, and the $E_{conformation}$ term referring to the difference between the energies of the isolated molecules in the bulk and in the vapor phase conformation. If we apply the above idea of lattice energy decomposition to two-dimensional (2-D) slices, we get,

$$E_{condensation}^{(hkl)} = E_{latt} - E_{conformation}^{(hkl)} \tag{3}$$

Using the fact that a slice has two surfaces,[16] the condensation energy is twice the attachment energy of a molecule to the crystal face,

$$E_{condensation}^{(hkl)} = 2E_{MAE}^{hkl} \tag{4}$$

Combining eq 3 and 4, we get following equation, which is similar to eq 1 for calculating molecular attachment energy, $E_{MAE}^{(hkl)}$,

$$E_{MAE}^{hkl} = \frac{1}{2}(E_{latt} - E_{molecule}^{hkl}) \tag{5}$$

where $E_{MAE}^{(hkl)}$ is energy released when a molecule gets adsorbed on the crystal face (hkl) from the vapor phase, but with the same conformation as in the slice, and $E_{molecule}^{hkl}$ is the difference between the energies of the isolated molecules on the slice and in the vapor phase conformation. The quantity of interest for morphological predictions is the MAE of all crystal face chosen for morphology prediction. This can then be related to the relative growth rate of that specific face under the hypothesis of eq 6 that the growth rate of a face is proportional to the MAE of the rate limiting molecule on the crystal faces:[5]

$$R_{rel,i} = \frac{R_i}{R_j} = \frac{E_{MAE}^{i}}{E_{MAE}^{j}} \tag{6}$$

Once the relative growth rates of all the chosen faces are known, a macroscopic image of the crystal morphology can be obtained from these energies by using the prescription of HP

dx.doi.org/10.1021/cg201047k | Cryst. Growth Des. 2012, 12, 732−741

model. The equilibrium shape can be constructed using a kinetic Wulff construction.[24] In accordance with this scheme, the distance r_{hkl} of a face (hkl) from the origin of the crystal is taken to be linearly related to the growth rate R_{hkl} of that face. The external shape of the crystal is determined by the lattice parameters, point group symmetry, miller index of the participating faces (hkl), and relative growth rate of faces.[25] Although for a given crystal lattice parameters and point group symmetry are fixed, the relative growth rate is a complex function of external (like supersaturation, temperature, solubility, etc.) and internal parameters (energetic of molecules in step at kink site in different faces and the molecular orientation in the case of a unit cell comprising more than one molecule). It should be noted that MAE of two similar molecules in a slice is not same; rather, it depends on relative orientation of molecules on the crystal face. The facet's growth is limited by the adsorption of molecules having the lowest MAE since the rate of growth is proportional to MAE.[5] However, the HP model always results in equal AE for each molecule in the facet's unit cell in spite of different relative orientations of molecules in the crystal faces.

The following methodology has been adopted to construct slices of different (hkl) from the projection of crystallographic structures of urea and succinic acid crystals. The charge neutrality of the slice is maintained during the process of slice generation. The origin is moved in order to minimize the number of symmetry operators with finite translation components. This is required before creating a slice from a three-dimensional crystal structure to maximize the symmetry operators. The slice must possess minimum energy configuration. If the molecule has a dipole moment, attention must be paid to the surface termination, because the slice can possess a net dipole perpendicular to the surface. The stability of the slice depends on its orientation, (hkl), number of atomic layers, correct surface termination and surface relaxation/reconstruction. The number of atomic layers in a slice is determined by the convergence of the surface energy, and in order to maintain the stoichiometry, we have taken all atomic layers contained in one slice of thickness d_{hkl}. While creating a slice, often more than one surface termination is possible. To identify the correct surface termination of the slice, the above-discussed criteria is used. In most cases, these conditions are satisfied at the same configuration.

The crystal surface that is taken as the starting point is not simply a straight cut from a zero temperature crystal structure, but the fraction of dismembered molecules is recombined to make them complete. Naturally, the resulting configuration is not favored energetically because, in molecular crystals, the molecular topology must be preserved and only intermolecular bonds are cut during the surface creation. The topology of dismembered molecules must be restored in order to obtain a stable surface configuration. To carry out molecular renovation of the dismembered molecules, we have calculated required displacements of the fragmented molecules using structural information such as bond lengths, bond angles, and dihedral angles. To elucidate the above procedure, we show in Figure 1a the (001) surface of urea crystal corresponding to the energetically unfavorable configuration which constitutes the fraction of incomplete and complete molecules. In order to integrate the dismembered molecule, each broken hydrogen atom needs to be displaced by 0.000 Å, −5.565 Å, and −4.680 Å along the X, Y, and Z direction, respectively. The configuration of the slice after the integration of the dismembered

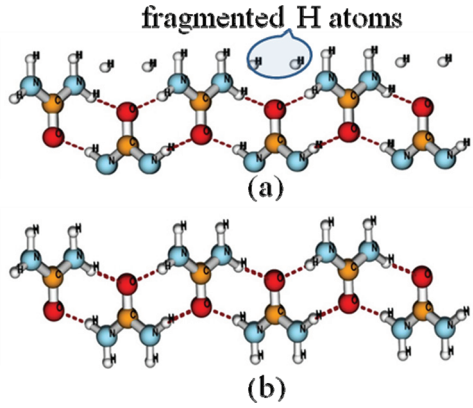

Figure 1. The structure of the (001) face of the urea crystal from (a) projection of the (001) plane from the crystal structure (b) after the integration of dismembered molecule in the projected plane.

molecule which is an energetically stable configuration is shown in Figure 1b. The surface configuration thus obtained for each face is further subjected to a geometry optimization procedure to obtain a relaxed slice structure. This is necessary because the ideal surface may undergo relaxation, without the loss of translational symmetry, or exhibit partial reconstruction.

Having discussed the procedure of creating slices, we next describe the method to calculate MAE of each molecule on the various crystal faces. Figure 2 shows typical urea molecules of

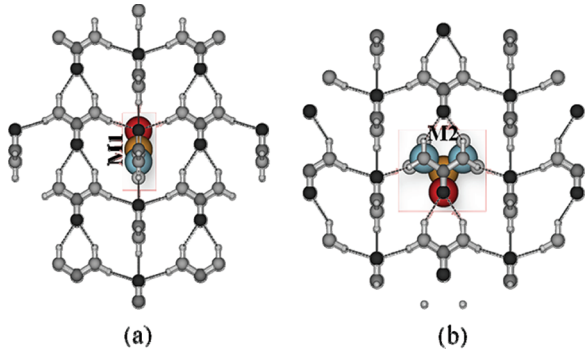

Figure 2. Schematic illustrations of urea molecules (color) in the (110) face of crystalline urea of (a) M1 and (b) M2 orientation in the presence of neighboring ghost atoms which are represented by gray balls.

M1 and M2 orientation on the (110) face of urea crystal. It is evident from Figure 2 that the arrangement of neighboring ghost atoms near M1 and M2 molecules are different. As a result of this MAE of M1 and M2 molecules on the (110) slice is not equal. The ghost atoms are points in space with an associated basis set, but lack a nuclear charge so allowing better description of the electron density in the vacancies. The number of distinct molecular orientation in a face is determined by the number of symmetrically unrelated molecules in the facet's 2-D unit cell. We have employed Hartree−Fock (HF) and density functional theory (DFT) with hybrid exchange-correlation functional (B3LYP) to obtain MAE of different faces of urea and succinic acid crystals.

3. COMPUTATIONAL DETAILS

Throughout this paper, we have carried out all calculations using CRYSTAL09 computer code.[26] The basis set employed for carbon,

dx.doi.org/10.1021/cg201047k | Cryst. Growth Des. 2012, 12, 732−741

Table 1. Experimental and Calculated Lattice Parameters and Lattice Energy of Urea and Succinic Acid Crystals Obtained from HF and DFT-B3LYP

			Hartree−Fock		DFT-B3LYP	
crystal		experimental lattice parameters[27,28] and sublimation enthalpy[30,31]		% dev		% dev
urea	*A*/Å	5.661	5.332	5.8	5.187	8.4
	C/Å	4.712	4.630	1.7	4.545	3.5
	lattice energy (kcal/mol)	−22.2	−21.0	5.4	−29.3	32.0
β-succinic-acid	*A*/Å	5.519	5.299	4.0	5.185	6.1
	B/Å	8.862	8.159	7.9	8.025	9.4
	C/Å	5.101	4.835	5.2	4.709	7.7
	β (deg)	91.59	97.38	6.3	98.77	7.8
	lattice energy (kcal/mol)	−30.8	−26.9	12.6	−37.1	20.5

nitrogen, and oxygen is s(6)sp(2)sp(1) and for the hydrogen atom it is s(2)s(1) ("6-21G"). The crystalline orbitals are represented as linear combinations of atom-centered Gaussian orbitals and are evaluated over a regular three-dimensional mesh in reciprocal space. Each Bloch function is built from atom-centered atomic orbitals, which are contractions (linear combinations with constant coefficient) of Gaussian-type functions (GTF), each GTF being the product of a Gaussian times a real solid spherical harmonic. The level of accuracy in evaluating the Coulomb and exchange series is controlled by five thresholds,[26] for which values of 10^{-10}, 10^{-10}, 10^{-10}, 10^{-10}, 10^{-20} are used for the Coulomb and exchange series. DFT exchange-correlation contribution is evaluated by numerical integration over the cell volume. The self-consistent-field-cycle (SCF) converges when the root-mean-square (rms) of the change in eigenvalues from two subsequent cycles is less than 10^{-10} hartree or the change in the absolute value of the total energy is less than 10^{-9} hartree. The shrinking factors along the reciprocal lattice vectors are set to 2, 2, 2, corresponding to eight reciprocal space points of the irreducible Brillouin zone at which the Hamiltonian matrix is diagonalized. To calculate the relaxed structure of bulk crystal and slices of different orientations, we start with experimental crystal structure[27,28] as the initial crystal structure. It should be mentioned that the most stable structure should be chosen as the initial structure in the case of more than one experimental structures are available. Following this we have chosen experimentally determined ground state structures of urea and succinic acid crystals as initial structures for lattice and molecular attachment energy calculations.

The lattice and atomic coordinates are fully relaxed by means of analytical gradients of the energy with respect to both cell parameters and atom coordinates. The geometry optimization is performed by means of a quasi-Newton optimization algorithm. Gradients are evaluated each time the energy is computed and the second derivative matrix is updated by means of the Broyden−Fletcher−Goldfarb−Shanno algorithm. At each step, a one-dimensional minimization using a quadratic polynomial is carried out, followed by an *n*-dimensional search using the Hessian matrix. Geometry convergence is tested on the rms and the absolute value of the largest component of the gradients and estimated displacements. The threshold for the maximum force, the rms force, the maximum atomic displacement, and the rms atomic displacement on all atoms have been set to 0.00045, 0.00030, 0.00180, and 0.00120 au, respectively. The symmetry is maintained during the all surface relaxation calculations. In order to check whether the optimized structure has reached equilibrium geometry or not, a stationary point on the potential energy surface is found where the total force acting on atoms is numerically zero. Geometry optimization is usually completed when the gradients are below a given threshold. In CRYSTAL09 code, the optimization convergence is checked on the rms and the absolute value of the largest component of both the gradients and the estimated displacements. When all conditions are satisfied simultaneously, the optimization process is considered to be complete.

Another issue connected with calculated lattice energy and MAE is the basis-set superposition error (BSSE). The BSSE arises because two molecules which are bound together make use of the basis function on the neighboring atoms to enhance the quality of their own basis sets over the quality used for the isolated molecule calculation. In fact, in calculating the total energy of a molecular crystal with a finite basis set, the description of molecule A in the crystal will be improved by the variational freedom provided by the functions of the adjacent molecule B, and vice versa. As a consequence, the energy content of A and B in the crystalline environment turns out to be overestimated, as if an extra binding occurred between A and B. This error is commonly corrected via the counterpoise (CP) method, as proposed by Boys and Bernardi,[29] by supplementing the basis set of an isolated molecule with the functions of an increasing number of ghost atoms belonging to the surrounding array of molecules that would be present in the crystal. For BSSE correction to the lattice energy, the monomer energy is calculated by placing ghost atoms in a cluster surrounding the monomer at the atomic positions obtained from the crystal structure optimization at the same computational level. The intramolecular energy is calculated by placing 89 ghost atoms in a cluster surrounding the molecule at the atomic positions obtained from the crystal structure optimization at the same computational level to calculate BSSE correction to the lattice energy and MAE. We have chosen 89 ghost atoms to calculate lattice energy of the above-mentioned crystals because the energies obtained are well converged and agree with the experimental results[30,31] as shown in Table 1. Our results reveal that the CP correction of urea crystal converges to a limiting value of about 9.1 kcal/mol with the largest calculation, which includes 89 ghost atoms. We note here that even inclusion of 30 neighbors is enough to reach a value of 8.5 kcal/mol that represents about 93% of the entire CP correction. The clusters of varying size containing a molecule of either M1 or M2 orientations in bulk and various faces of urea and succinic acid crystals are generated. To carry out CP correction, all the functions of the neighboring atoms in the crystals/faces are added to the basis set of the selected molecule (s) such that the following two criteria are obeyed: (i) the atom is within a distance *R* less than R_{max} (maximum distance explored while searching the neighbors of the atoms belonging to the molecule (s)) from at least one atom in the molecule and (ii) the atom is within the *N*th nearest neighbors of at least one atom in the molecule.

The size of the generated cluster is determined by R_{max} and number of nearest neighbors included into the calculation. For instance, calculation of lattice energy of urea crystal with the largest number of ghost atoms (89) corresponds to R_{max} = 5 Å and 30 nearest neighbors. All atoms in the generated cluster are converted into ghost atoms except for the atoms of the label molecule to calculate lattice and molecular attachment energies for different faces of urea and succinic acid crystals. Figure 2 shows urea molecule in the (110) face of urea crystal with M1 (a) and M2 (b) orientations in the presence of neighboring ghost atoms. The ghost atoms are represented by gray balls, while the atoms of the label molecule having orientations M1 and M2 are shown by colored balls. Furthermore, the structural optimization of a single molecule of each compound in M1 and M2 orientations within the presence of neighboring ghost atoms are also performed so that the possible energy reduction due to conformational change of the molecule from the solid state to the gas phase could be

dx.doi.org/10.1021/cg201047k | Cryst. Growth Des. 2012, 12, 732−741

considered. It is required in order to calculate relaxed MAE of different faces of urea and succinic acid crystals.

4. RESULTS AND DISCUSSION

The accurate calculation of hydrogen bonding (HB) in the molecular crystals pose a problem to study the stability of these crystals. We have performed ab initio calculations which in principle take care of HB. However, because of the approximate nature of the exchange-correlation potential involved in the calculations, it does not accurately reproduce the HB in the molecular and other weakly bonded crystals such as urea and succinic acid crystals. To address this shortcoming of the ab initio calculations, we have employed the post self-consistent field (SCF) method[29,32,33] to recover HB energy and dispersion energy in molecular crystals. It has already been demonstrated that the BSSE plays an important role in binding of weakly interacting molecules. Ordinary BSSE tends to cancel the lack of dispersive interactions in small and moderate basis sets. BSSE leads to an overestimation of the interaction energies. On the other hand, the use of full BSSE correction is questionable, since it may lead to a spurious overcorrection.[34] Kim et al.[35] have studied the different proportions of BSSE correction on the binding energies of weakly bound π-complexes and found that 50% BSSE correction yields reasonably accurate interaction energies, especially with moderate basis sets. We apply this idea to compute lattice energies of above-mentioned molecular crystals and found that it is useful to employ a 50% BSSE correction when comparing the theoretically evaluated quantities such as lattice energies, and enthalpies with the experimentally determined ones. It should be mentioned that the 50% BSSE correction cannot be theoretically justified. However, in the particular case of calculations of large molecular complexes with moderate basis sets, the methods often yield good results because the ordinary BSSE tends to cancel the lack of dispersive interactions in small and moderate basis sets. With the small basis sets, the BSSE gives an extra-binding that compensates for the missing dispersion forces, thus yielding structures and energy in fortuitous agreement with experiments.

The role of BSSE in accounting for the hydrogen bond has been studied for water dimer, and it has been established that the binding energy obtained using HF approximation and employing small basis set is in good agreement with the experimental results.[36] On the other hand, DFT-B3LYP calculations with moderate size of basis set give better binding energy of water dimer than the HF method.[36] Dobado et al.[37] and Civalleri et al.[33] have studied the lattice energies of crystalline urea, using the DFT-B3LYP method and demonstrated that the results obtained with the B3LYP functional is able to accurately produce the HB energy. In view of this, we have employed HF and DFT-B3LYP methods for our present calculations. It is well established that relatively smaller basis sets perform better in periodic than in molecular calculations.[32] Moreover, Civalleri et al.[33] have calculated structure and lattice energy of urea crystal using moderate to large basis sets and demonstrated that when large basis sets were employed, the discrepancy between experimental and computational results increases. Keeping this in mind, we have employed relatively smaller basis set, in order to obtain HB energy and dispersion energy in crystalline urea and succinic acid crystals, by employing 50% BSSE corrections. The present calculations were performed at 0 K; thus we have ignored the entropic contribution to obtain the habit controlling energetic. The effect of temperature and different surface configurations on growth shape can be studied by performing complex molecular dynamic simulation which is beyond the scope of this paper. We are currently investigating the effect of temperature and other external growth factors affecting crystal growth shape using kinetics of the growth processes through which assembly occurs. Details will be published in due course of time.

We begin with the discussion on the dependence of a different proportion of BSSE correction on lattice energy of urea crystal as a function of the number of neighboring atoms included in the CP correction for crystalline urea, with HF and DFT-B3LYP using the 6-21G basis set. These results are displayed in Figure 3. The experimental and calculated lattice

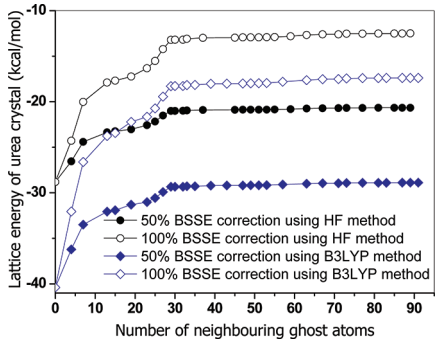

Figure 3. Dependence of different proportions of BSSE correction on the lattice energy of urea crystal as a function of neighboring ghost atoms, with HF and DFT-B3LYP using the 6-21G basis set.

parameters and lattice energies of urea and succinic acid crystals obtained from HF and DFT-B3LYP calculations are presented in Table 1. It is evident from Table 1 that the calculated lattice energies and lattice parameters of these crystals obtained using the HF method are in better agreement with the experimental enthalpy of sublimation.[30,31] The results for % deviation in lattice parameters and lattice energy clearly show that the values obtained from the HF method are in close agreement with the corresponding experimental result compared to the result obtained using the DFT-B3LYP method. We have also considered a relatively larger basis set (6-31G(d,p) and 6-311G(d,p) basis sets) to study the effect of BSSE on lattice energies of the above-mentioned crystals. We found a negligible dependence on the basis set used, although the BSSE correction decreases with the size of basis. However, use of the larger basis sets leads to a drastic increase in the computational time. Keeping this in mind, we have employed 50% BSSE correction and moderate basis set (6-21G) to calculate lattice energies and MAE of M1 and M2 molecules in various faces of urea and succinic acid crystals.

Having discussed the effect of BSSE on lattice energies, we now turn to discuss the results of the MAE of M1 and M2 molecules in urea and succinic acid crystals. First, we study the equilibrium morphology of urea crystal. In order to predict the growth shape of a crystal, we start with selection of the set of candidate planes. The accurate prediction of crystal shape requires correct selection of slow growing planes which are important in crystal growth. We have considered nine low-index faces for calculating MAE of molecules. Out of these nine faces three are chosen to have slightly higher index faces as compared to the remaining six faces. These nine faces are slow growing faces and correspond to higher interplanar spacing and

dx.doi.org/10.1021/cg201047k | Cryst. Growth Des. 2012, 12, 732–741

Table 2. Parameters Used for Construction of Various Slices of Urea Crystal

face	number of atomic layer	label of surface atom	label of the dismembered molecules	is the face coplanar?	label of rate determining molecule
(100)	14	3(O),5(N), 10(H),12(H)	M2	yes	both M1 and M2
(110)	7	2(C), 7(N)	M2	no	M1
(101)	16	4(O)	none	yes	both M1 and M2
(001)	10	2(C), 10(H)	M2	yes	both M1 and M2
(111)	13	5(N)	M1	no	M2
(210)	14	7(N), 8(N)	M2	no	M1
(201)	16	1(C)	both M1 and M2	yes	both M1 and M2
(211)	16	6(N), 7(N)	M1	no	M2

Table 3. Unrelaxed and Relaxed $E^{hkl}_{molecule}$ and E^{hkl}_{MAE} (kcal/mol) of M1 and M2 Orientated Molecules in Different Faces of Urea Crystal

		unrelaxed $E^{hkl}_{molecule}$ (kcal/mol) of orientation		unrelaxed E^{hkl}_{MAE} (kcal/mol) of orientation		relaxed $E^{hkl}_{molecule}$ (kcal/mol) of orientation		relaxed E^{hkl}_{MAE} (kcal/mol) of orientation	
Hamiltonian	face (*hkl*)	M1	M2	M1	M2	M1	M2	M1	M2
HF	(200)	−7.23		−7.03		−11.29		−5.00	
	(110)	−12.14	−6.31	−4.58	−7.49	−15.54	−10.52	−2.88	−5.39
	(101)	−4.63	−4.63	−8.33	−8.33	−8.84	−8.84	−6.23	−6.23
	(001)	−8.94	−8.94	−6.17	−6.17	−12.38	−12.38	−4.46	−4.46
	(111)	−1.33	−9.08	−9.98	−6.11	−6.00	−12.36	−7.65	−4.47
	(100)	−9.26	−9.26	−6.02	−6.02	−13.06	−13.06	−4.12	−4.12
	(210)	−8.94	−5.98	−6.18	−7.66	−12.73	−10.19	−4.28	−5.55
	(201)	−1.29	−1.29	−10.00	−10.00	−6.00	−6.00	−7.65	−7.65
	(211)	−1.01	−5.10	−10.14	−8.10	−5.68	−10.76	−7.81	−5.27
B3LYP	(200)	−8.15		−9.43		−11.18		−7.92	
	(110)	−13.27	−7.10	−6.87	−9.95	−15.71	−10.30	−5.65	−8.35
	(101)	−4.66	−4.66	−11.18	−11.18	−7.89	−7.89	−9.56	−9.56
	(001)	−9.31	−9.31	−8.85	−8.85	−12.07	−12.07	−7.47	−7.47
	(111)	−1.08	−9.47	−12.96	−8.77	−4.67	−11.84	−11.17	−7.58
	(100)	−10.13	−10.13	−8.44	−8.44	−12.95	−12.95	−7.03	−7.03
	(210)	−9.76	−6.65	−8.62	−10.18	−12.57	−9.82	−7.22	−8.59
	(201)	−1.23	−1.23	−12.89	−12.89	−4.85	−4.85	−11.08	−11.08
	(211)	−0.85	−5.22	−13.08	−10.89	−4.44	−8.34	−11.28	−9.33

are expected to appear in the equilibrium morphology. In Table 2 we list all the parameters which have been used for constructing these nine slices uniquely. We need to restore the integrity of dismembered molecules, as mentioned in methodology section, for all the slices except for the (101) face. The results for the unrelaxed and relaxed MAE of these faces are compiled in Table 3. Figure 4 shows the optimized structures of different faces of urea crystal. It is clear from Figure 4 and Tables 2 and 3 that both M1 and M2 molecules in (100), (101), (001), and (201) slices have equal MAE signifying that the molecules lie on the same plane. The growth of these faces is determined equally by the adsorption of M1 and M2 molecules. On the other hand, for (110), (111), (210), and (211) MAE of M1 and M2 are unequal resulting from their non-coplanar structure. The growth of (110) and (210) faces are determined by the adsorption of M1 molecule as MAE of M1 is lower than M2. In contrast to this, growth of (111) and (211) are limited by the adsorption of M2 molecule as MAE of M2 is lower than M1.

In Figure 5 we show the shapes of urea crystal ((a−c) unrelaxed and (b−d) relaxed) obtained by using HF and DFT-B3LYP, respectively. It is evident from Figure 5 that the morphologies of urea calculated using the DFT-B3LYP method show the appearance of (200) and (101) faces, but they are absent from the experimental morphology.[11] It can also be seen from Figure 5 that the morphologies obtained using the HF

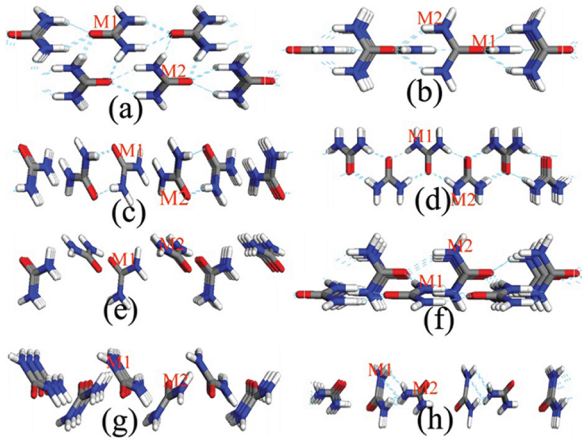

Figure 4. Relaxed slice structure of urea crystal of orientation (a) (100), (b) (110), (c) (101), (d) (001), (e) (111), (f) (210), (g) (201), and (h) (211).

method correctly predicts all experimentally observed faces in the urea crystal. A comparison with a shape drawn from a scanning electron micrograph of urea crystallized from the vapor phase[11] as shown in Figure 6 reveals that there is an excellent agreement between our calculated relaxed morphology using HF method and the experimental results for vapor

dx.doi.org/10.1021/cg201047k | Cryst. Growth Des. 2012, 12, 732−741

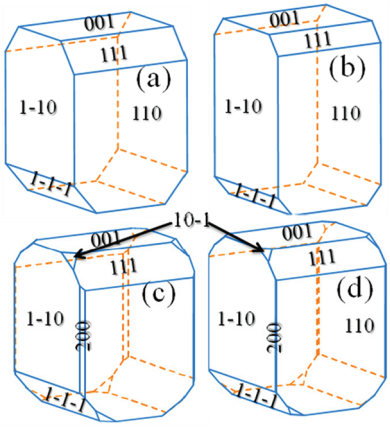

Figure 5. Calculated equilibrium morphologies of crystalline urea (a–c) unrelaxed and (b–d) relaxed structure from the HF and DFT-B3LYP method, respectively.

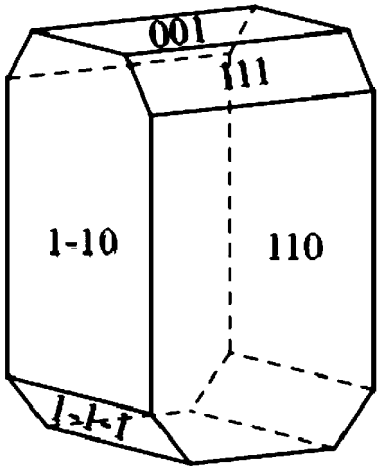

Figure 6. The experimental growth shape of crystalline urea from vapor, reproduced with permission from Docherty et al.[11] Copyright 1993 Royal Society of Chemistry.

grown crystals. However, it should be noted that relaxed shape of urea crystal obtained from HF calculation (Figure 5b) appears to be stretched out. This can be explained on the basis of a large change in MAE when the rate limiting molecule is relaxed on the different faces of urea crystal. For example, corresponding to (110) face of urea crystal (Table 3), the adsorption of M1 molecule to the (110) face is rate limiting. The % difference between the relaxed and unrelaxed MAE of M1 molecule to the (110) face of urea crystal using HF and DFT-B3LYP methods are 37% and 18%, respectively. This large change in the MAE for HF calculation causes stretching of the crystal shape. The % change in MAE of rate limiting molecules in different faces of urea crystal is presented in Table 4 which clearly shows for the HF method the percentage change in MAE is approximately two times more than that of the DFT-B3LYP method. Nevertheless, the equilibrium shape of urea crystal obtained using HP does not resemble the experimental observation.[10,15]

Having discussed the results for the equilibrium morphology of urea crystal, we next focus our attention on the study of morphology of succinic acid crystal. To this end, we consider eight low-index faces for calculating MAE. In Figure 7, we show the optimized structures of different faces of succinic acid crystal. All the parameters used for constructing the above-mentioned

Table 4. % Changes in MAE of Rate Limiting Molecules in Different Faces of Urea Crystal Using HF and DFT-B3LYP Methods

face (*hkl*)	% difference between the relaxed and unrelaxed MAE of rate limiting molecule using	
	HF	DFT-B3LYP
(200)	28.9	16.0
(110)	37.1	17.8
(101)	25.2	14.5
(001)	27.7	15.6
(111)	26.8	13.6
(100)	31.6	16.7
(210)	30.7	16.2
(201)	23.5	14.0
(211)	34.9	14.3

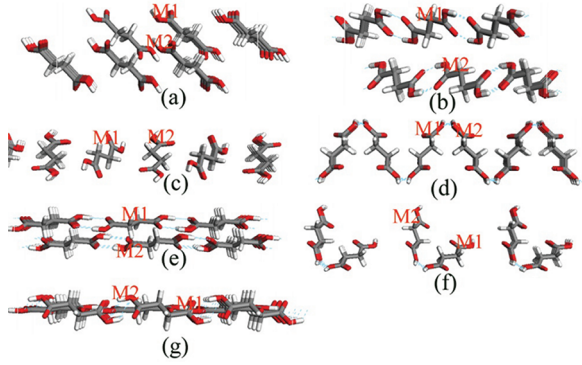

Figure 7. Relaxed slice structure of succinic acid crystal of orientation (a) (001), (b) (010), (c) (011), (d) (100), (e) (101), (f) (110), and (g) (111).

slices are listed in Table 5. In Table 6, we report the unrelaxed and relaxed MAE of M1 and M2 molecules in the slices of succinic acid crystal. It is clear from Figure 7 and Tables 5 and 6 that both M1 and M2 molecules in (001), (010), and (101) slices have same MAE as they have a coplanar structure. The growth of these faces is determined by the adsorption of M1 and M2 molecules equally. On the other hand (011), (100), (110), and (111) slices show non-coplanar structure and MAE of M1 and M2 molecules are unequal. The growth of (011), (110), and (111) faces are determined by the adsorption of M1 molecule as MAE of M1 is lower than M2. On the other hand, growth of the (100) face is limited by the adsorption of the M2 molecule as than MAE of M2 is lower than that of M1.

Using the results presented in Table 6, growth morphologies of succinic acid crystal has been drawn. These are shown in Figure 8 ((a–c) unrelaxed and (b–d) relaxed) obtained by using HF and DFT-B3LYP methods. It is clear from Figure 8 that the morphology of succinic acid crystal calculated using the DFT-B3LYP method show the appearance of the (002) face, but it is distinctly absent in the experimental morphology.[16−18] On the other hand, the relaxed shape of succinic acid crystal calculated from the HF method (see Figure 8b) is in good agreement with the experimentally grown crystal. A comparison with a shape drawn from the vapor phase of succinic acid,[18] as shown in Figure 9, reveals that there is good agreement between our calculated relaxed shape obtained using the HF method and the experimental results. In Table 7 we compare the % change of MAE of rate limiting molecule in different faces of succinic

dx.doi.org/10.1021/cg201047k | Cryst. Growth Des. 2012, 12, 732–741

Table 5. Same as Table 2 but for β-Succinic Acid Crystal

face	number of atomic layer	label of surface atom	label of the dismembered molecules	is the face coplanar?	label of rate determining molecule
(001)	28	3(C),13(O), 17(H),27(H)	M2	yes	both M1 and M2
(010)	28	8(C), 22(H)	none	yes	both M1 and M2
(011)	28	14(O)	M1	no	M1
(100)	14	7(C), 9(O)	M2	no	M2
(101)	28	7(C), 9(O)	M2	yes	both M1 and M2
(110)	28	15(O)	M2	no	M1
(111)	26	14(O)	none	no	M1

Table 6. Unrelaxed and Relaxed $E^{hkl}_{molecule}$ and E^{hkl}_{MAE} (kcal/mol) of M1 and M2 Molecules of Different Faces of Succinic Acid Crystal

		unrelaxed $E^{hkl}_{molecule}$ (kcal/mol) of orientation		unrelaxed E^{hkl}_{MAE} (kcal/mol) of orientation		relaxed $E^{hkl}_{molecule}$ (kcal/mol) of orientation		relaxed E^{hkl}_{MAE} (kcal/mol) of orientation	
Hamiltonian	face (*hkl*)	M1	M2	M1	M2	M1	M2	M1	M2
HF	(002)	−1.49		−11.66		−1.75		−11.53	
	(010)	−8.00	−8.00	−8.40	−8.40	−9.79	−9.79	−7.51	−7.51
	(011)	−4.73	−4.17	−10.04	−10.32	−5.13	−4.91	−9.84	−9.94
	(020)	−9.08		−7.86		−10.37		−7.22	
	(100)	−8.25	−8.25	−8.28	−8.28	−12.84	−14.68	−5.98	−5.06
	(101)	−8.97	−8.94	−7.92	−7.93	−10.93	−10.93	−6.94	−6.94
	(110)	−6.06	−5.35	−9.37	−9.73	−9.73	−8.03	−7.54	−8.39
	(111)	−10.68	−9.45	−7.06	−7.68	−12.45	−11.64	−6.18	−6.58
B3LYP	(002)	−0.01		−16.57		−0.78		−16.18	
	(010)	−8.08	−8.08	−12.53	−12.53	−9.62	−9.62	−11.76	−11.76
	(011)	−3.22	−2.47	−14.96	−15.34	−4.51	−3.15	−14.32	−15.00
	(020)	−9.39		−11.88		−10.76		−11.19	
	(100)	−7.97	−7.97	−12.59	−12.59	−12.11	−15.46	−10.52	−8.84
	(101)	−9.10	−9.07	−12.02	−12.04	−10.98	−10.98	−11.08	−11.08
	(110)	−5.03	−4.19	−14.06	−14.48	−9.06	−7.40	−12.04	−12.87
	(111)	−11.16	−9.95	−10.99	−11.60	−12.86	−12.03	−10.14	−10.56

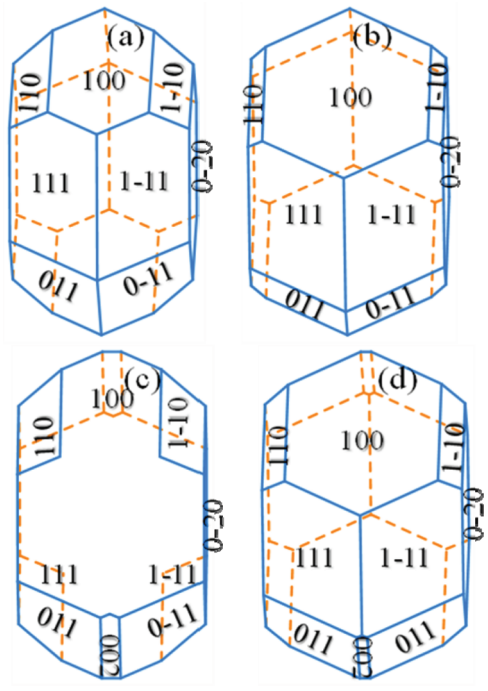

Figure 8. Calculated equilibrium morphologies of β-succinic acid crystal (a−c) unrelaxed and (b−d) relaxed structure from the HF and DFT-B3LYP method, respectively.

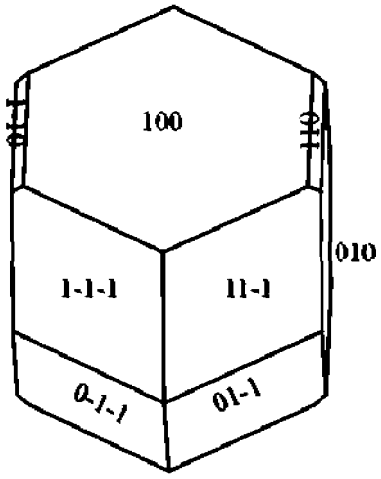

Figure 9. The experimental growth shape of β-succinic acid crystal from vapor, reproduced with permission from Elly van der Voort.[18] Copyright 1991 Elsevier.

acid crystal using the HF and DFT-B3LYP method. It clearly shows that, unlike urea crystal, no definite trend is observed for succinic acid crystal and this is also reflected in Figure 8.

It is interesting to re-examine the physical picture of the HP model and the MAE-based approach proposed here for the

dx.doi.org/10.1021/cg201047k | Cryst. Growth Des. 2012, 12, 732−741

Table 7. % Changes in MAE of Rate Limiting Molecules in Different Faces of Succinic Acid Crystal Using HF and DFT-B3LYP Methods

face (*hkl*)	% difference between the relaxed and unrelaxed MAE of rate limiting molecule using	
	HF	DFT-B3LYP
(002)	1.1	2.3
(010)	10.6	6.1
(011)	2.0	4.3
(020)	8.1	15.6
(100)	38.8	29.8
(101)	12.4	7.8
(110)	19.5	14.4
(111)	12.5	7.7

morphology prediction from the vapor phase. It is well-known that in crystal growth studies the crystal surface plays an important role. The HP model assumes that the surface is a perfect termination of the bulk and that no surface rearrangement has taken place. This has been shown to have a significant effect in the cases of inorganic[38] and organic[10,15] systems. In the crystal graph theory[4] which is an extension of HP model, the bulk crystal structure is also used to model the structure of the surface, thereby neglecting surface relaxations and surface reconstructions. Thus, connected nets are specific bulk terminations of the crystalline materials. In the case of anisotropic crystals, the adsorption energy of growth units depends on the relative orientation of growth units at the surface which is also not taken into account in the HP model. In the present paper, we have extended the capability of HP model by considering the role of molecular orientation of growth units in the case of unit cell comprising more than one growth unit and surface relaxation to predict the shape of molecular crystals. Our results show that the predictive power of the HP model can be improved by considering the effect of molecular orientation and surface relaxation. The growth mechanism of real crystals such as urea and succinic acid, however, usually have more complex structures, often with more than one growth unit in the unit cell and with different bonds, resulting in various step configurations. The crystal growth of these crystals involves multiple growth unit incorporation barriers, different for each incorporation site configuration. Also, the order in which the different growth units incorporate affects the overall energetic profile, and multiple pathways to the same structure can have very different energetics associated with them.

We close this section by commenting on the uneven growth of (111) and its Freidel opposite $(\overline{1}\overline{1}\overline{1})$ faces of the urea crystal. We have calculated MAE of these faces before and after relaxation. However, we do not find any difference in MAE of the two faces. Self-poisoning model[39] has been proposed to address the uneven growth of (011) and $(0\overline{1}\overline{1})$ faces of α-resorcinol crystal from the vapor phase. However, experimental verification of the self-poisoning model is difficult to devise. To discriminate the habit controlling energetics of the two above-mentioned faces, we are presently carrying out calculations of step energies taking into account the orientations of urea molecules. Our results reveal that the anomalous growth of (111) and $(\overline{1}\overline{1}\overline{1})$ faces of urea crystal is a fundamental characteristic of the growth of urea crystal. Results of this study will be published in due course of time.

5. SUMMARY AND CONCLUSIONS

In summary, we have calculated equilibrium shapes of molecular crystals by performing periodic ab initio total energy calculation in order to obtain adsorption energy of molecules on the different faces. The effect of molecular orientation and surface relaxation on equilibrium morphology has been studied. The calculated equilibrium morphologies of urea and succinic acid crystals show excellent agreement with the experimentally grown crystals by the vapor phase. In both cases, the calculated morphologies reproduced all the experimentally observed faces which clearly demonstrate the validity of the discussed model.

AUTHOR INFORMATION

Corresponding Author

*Phone +91-731-248-8677. E-mail: mksingh@rrcat.gov.in.

ACKNOWLEDGMENTS

The authors are grateful for the support and motivation received from Dr. V. K. Wadhawan. Discussions with S. K. Sharma and Prof. Julian Gale are gratefully acknowledged. The referees for this paper are also thanked for their helpful comments. All the calculations were performed on Brahma and Nalanda Linux clusters at our centre.

REFERENCES

(1) Smith, C. S. In *A Search for Structure; Selected Essays on Science, Art, and History*; MIT Press: Cambridge, MA, 1981.
(2) (a) Bravais, A. *Etudes Cristallographiques*; Gauthier-Villars: Paris, France, 1866. (b) Friedel, G. *Bull. Soc. Franc. Mineral.* **1907**, *30*, 326–455. (c) Donnay, J. D. H.; Harker, D. *Am. Mineral.* **1937**, *22*, 446–467.
(3) (a) Hartman, P.; Perdok, W. G. *Acta Crystallogr.* **1955**, *8*, 49–52. (b) Hartman, P. In *Crystal Growth: An Introduction*; Hartman, P., Eds.; North Holland: Amsterdam, 1973; Chapter 14, pp 367–402.
(4) (a) Bennema, P. In *Handbook of Crystal Growth*; Hurle, D. T. J., Eds.; Elsevier Science Publishers: Amsterdam, 1993; Vol. *1a*, Chapter 7, pp 477–581. (b) Hartman, P.; Bennema, P. *J. Crystal Growth* **1980**, *49*, 145–156.
(5) Berkovitch-Yellin, Z.; van Mil, J.; Addadi, L.; Idelson, M.; Lahav, M.; Leiserowitz, L. *J. Am. Chem. Soc.* **1985**, *107*, 3111–3122.
(6) Lahav, M.; Leiserowitz, L. *Chem. Eng. Sci.* **2001**, *56*, 2245–2253.
(7) (a) Liu, X. Y.; Boek, E. S.; Briels, W. J.; Bennema, P. *Nature* **1995**, *374*, 342–345. (b) Liu, X. Y.; Bennema, P. *Phys. Rev. B* **1994**, *49*, 765–775. (c) Liu, X. Y.; Boek, E. S.; Briels, W. J. *J. Chem. Phys.* **1995**, *103*, 3747–3754. (d) Liu, X. Y.; Bennema, P. *Phys. Rev. B* **1996**, *53*, 2314–2325. (e) Liu, X. Y. *Phys. Rev. B* **1999**, *60*, 2810–2817.
(8) De Vries, S. A.; Goedtkindt, P.; Bennett, S. L.; Huisman, W. J.; Zwanenburg, M. J.; Smilgies, D.-M.; De Yoreo, J. J.; van Enckevort, W. J. P.; Bennema, P.; Vlieg, E. *Phys. Rev. Lett.* **1998**, *80*, 2229–2232.
(9) Strom, C. S. *J. Cryst. Growth* **2001**, *222*, 298–310.
(10) George, A. R; Harris, K. D. M.; Rohl, A. L.; Gay, D. H. *J. Mater. Chem.* **1995**, *5*, 133–139.
(11) (a) Docherty, R.; Roberts, K. J.; Saunders, V.; Black, S.; Davey, R. J. *Faraday Discuss.* **1993**, *95*, 11–25. (b) Feigelson, R. S.; Route, R. K.; Kao, T.-M. *J. Cryst. Growth* **1985**, *72*, 585–594.
(12) Boek, E. S.; Feil, D.; Briels, W. J.; Bennema, P. *J. Cryst. Growth* **1991**, *114*, 389–410.
(13) Bisker-Leib, V.; Doherty, M. F. *Cryst. Growth Des.* **2001**, *1*, 455–461.
(14) Engkvist, O.; Price, S. L.; Stone, A. J. *Phys. Chem. Chem. Phys.* **2000**, *2*, 3017–3027.
(15) Singh, M. K.; Banerjee, A. *Cryst. Res. Tech.* **2011**, *46*, 1035–1043.
(16) Berkovitch-Yellin, Z. *J. Am. Chem. Soc.* **1985**, *107*, 8239–8253.
(17) Docherty, R.; Roberts, K. J. *J. Crystal Growth* **1988**, *88*, 159–168.
(18) van der Voort, E. *J. Cryst. Growth* **1991**, *110*, 662–668.

(19) Rohl, A. L.; Gay, D. H. *J. Crystal Growth* **1996**, *166*, 84−90.
(20) Borc, J.; Sangwal, K. *Surf. Sci.* **2004**, *555*, 1−10.
(21) Jiang, X. N.; Xu, D. *J. Appl. Crystallogr.* **2003**, *36*, 1448−1451.
(22) Nangia, A. In *Models, Mysteries and Magic of Molecules*; Boeyens, J. C. A. Ogilvie, J. F., Eds.; Springer, The Netherlands, 2008; Chapter 3, pp 63−86.
(23) Dovesi, R.; Civalleri, B; Orlando, R.; Roetti, C.; and Saunders, V. R. In *Reviews in Computational Chemistry*; Lipkowitz, K. B.; Larter, R; and Cundari, T. R., Eds.; John Wiley & Sons, Inc.: New York, 2005; Vol. *21*, Chapter 1, pp 49.
(24) Wulff, G. *Z. Kristallogr.* **1901**, *34*, 449−530.
(25) http://www.shapesoftware.com.
(26) (a) Dovesi, R.; Orlando, R.; Civalleri, B.; Roetti, R.; Saunders, V. R.; Zicovich- Wilson, C. M. *Z. Kristallogr.* **2005**, *220*, 571−573. (b) Dovesi, R.; Saunders, V. R.; Roetti, R.; Orlando, R.; Zicovich-Wilson, C. M.; Pascale, F.; Civalleri, B.; Doll, K.; Harrison, N. M.; Bush, I. J.; D'Arco, P.; Llunell, M. *CRYSTAL09 (CRYSTAL09 User's Manual)*; University of Torino: Torino, 2009.
(27) Swaminathan, S.; Craven, B. M.; McMullan, R. K. *Acta Crystallogr. Sect. B.* **1984**, *40*, 300−306.
(28) Broadley, J. S.; Cruickshank, D. W. J.; Morrison, J. D.; Robertson, J. M.; Shearer, H. M. M. *Proc. R. Soc. London, Ser. A* **1959**, *251* (No. 1267), 441−457.
(29) Boys, S. F.; Bernardi, F. *Mol. Phys.* **1970**, *19*, 553−559.
(30) Cox, J. D.; Pilcher, G. In *Thermochemistry of Organic and Organometallic Compounds*; Academic Press: New York, 1970.
(31) Momany, F. A.; Carruthers, L. M.; McGuire, R. F.; Scheraga, H. A. *J. Phys. Chem.* **1974**, *78*, 1595−1620.
(32) Dovesi, R.; Civalleri, B.; Orlando, R.; Roetti, C.; Saunders, V. R. *Rev. Comput. Chem.* **2005**, *21*, 1−125.
(33) Civalleri, B.; Doll, K.; Zicovich-Wilson, C. M. *J. Phys. Chem. B.* **2007**, *111*, 26−33.
(34) (a) Johansson, A.; Kollman, P.; Rotherberg, S. *Theor. Chim. Acta* **1973**, *29*, 167−172. (b) Daudey, J. P.; Claverieand, P.; Malrieu, J. P. *Int. J. Quantum Chem.* **1974**, *8*, 1−15.
(35) Kim, K. S.; Tarakeshwar, P.; Lee, J. Y. *Chem. Rev.* **2000**, *100*, 4145−4185.
(36) Koch, W.; Holthausen, M. C. In *A Chemist's Guide to Density Functional Theory*; Wiley-VCH Press: Cambridge, MA, 1981; pp 217−238.
(37) Dobado, J. A.; Molina, J.; Portal, D. *J. Phys. Chem. A* **1998**, *102*, 778−784.
(38) Mackrodt, W. C.; Davey, R. J.; Black, S. N.; Docherty, R. *J. Cryst. Growth* **1987**, *80*, 441−446.
(39) Weissbuch, I.; Leiserowitz, L.; Lahav, M. *Cryst. Growth Des.* **2006**, *6*, 625−628.